

Nitride Electrode Stoichiometry Effects on Ferroelectric Response in Hafnium Zirconium Oxide Thin Films

Jon F. Ihlefeld^{1,2,*}, Shelby S. Fields¹, Sean W. Smith³, Steven Wolfley³, M. David Henry³, Maria G. Sales¹, Samantha T. Jaszewski¹, Stephen J. McDonnell¹, Chris M. Fancher⁴, and Paul S. Davids³

¹Department of Materials Science and Engineering, University of Virginia, Charlottesville, Virginia 22904, USA

²Department of Electrical and Computer Engineering, University of Virginia, Charlottesville, Virginia, 22904, USA

³Sandia National Laboratories, Albuquerque, New Mexico, 87185, USA

⁴Oak Ridge National Laboratory, Oak Ridge, Tennessee, 37830, USA

*e-mail: jihlefeld@virginia.edu

Film stress is a known factor in the stability of the ferroelectric phase in hafnium oxide-based ferroelectrics. In this work, we explore the impact of electrode processing conditions on ferroelectric response in 20 nm thick hafnium zirconium oxide (HZO) thin films of nominal composition of $\text{Hf}_{0.5}\text{Zr}_{0.5}\text{O}_2$. RF magnetron sputtered TaN electrodes with varying stress states will be shown to impact the polarization response of the HZO films. It will be shown that while stress is a contributor to the polarization response, electrode stoichiometry appears to have a significant impact. TaN electrodes that are tantalum-rich result in HZO films with the largest polarization responses. Scavenging of oxygen by the non-stoichiometric HZO electrodes and resulting oxygen vacancy formation in the HZO films is suggested to be the mechanism leading to large polarizations.

Key words: hafnia, stress, stoichiometry, thin film

1. INTRODUCTION

The report of ferroelectricity in silicon-doped hafnium oxide thin films in 2011¹ has spurred a tremendous amount of interest into this and related materials as they offer potential solutions to a number of technologies, such as negative differential capacitance transistors, ferroelectric field effect transistors, and highly scaled ferroelectric memory. It is the inherent silicon compatibility² and scalable processing methods, such as atomic layer deposition, that leads to such promise.

Ferroelectricity in hafnium-oxide based materials is attributed to the switchable permanent dipole moment in a metastable orthorhombic $Pca2_1$ phase.¹ This phase does not appear on any equilibrium phase diagram and its stability with respect to the room temperature equilibrium monoclinic and high temperature tetragonal phases is influenced by a number of factors. These factors include: dopants, such as Si,³ La,⁴ Gd,⁵ and Y⁶ and alloys, such as $\text{HfO}_2\text{-ZrO}_2$ ⁷ and $\text{HfO}_2\text{-CeO}_2$;⁸ surface energies lowering the overall free energy,⁹ which necessitates thin films and/or fine grain sizes; stress, where biaxial tensile stresses favor orienting the short polar axis out of plane;¹⁰ and oxygen vacancies,¹¹ where high oxygen vacancy concentrations increase stability of higher symmetry phases. Included in the oxygen vacancy stability argument is the effect of electrodes on polarization response. It has been shown that more reactive electrodes, such as TaN, result in higher remanent polarizations than less reactive electrodes, such as TiN.⁵ It should be noted that several of these general ferroelectric phase stabilizing parameters are not universally accepted. Recently, micron-scale thickness films have been prepared with Y-doped HfO_2 ,¹² which suggests that nanoscale thicknesses or grain sizes may not be necessary. Switchable

polarizations have also been observed in pure HfO_2 and ZrO_2 and demonstrate that doping and/or alloying is not always needed to form the ferroelectric phase.^{13,14}

Of interest in this work is the role of processing on stabilizing the ferroelectric phase. This is motivated by the observation of large differences in ferroelectric polarization in films that have nominally identical structures (compositions and ferroelectric film thickness) where the oxide has been prepared by nominally identical deposition methods (atomic layer deposition) and submitted to nominally identical crystallization annealing temperatures. This is exemplified in Figure 1 for ~10 nm thick $\text{Hf}_{0.5}\text{Zr}_{0.5}\text{O}_2$ films with TiN electrodes.^{7, 15-17}

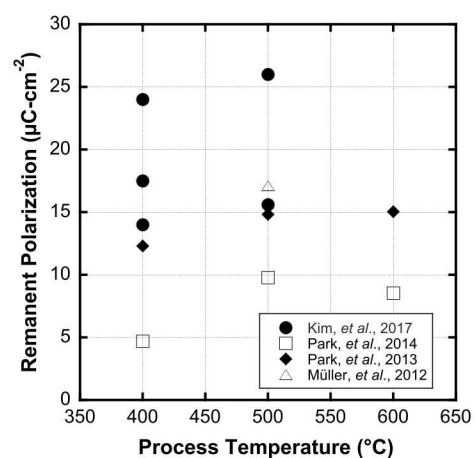


Fig. 1: Comparison of remanent polarization for nominally identical 10 nm thick $\text{Hf}_{0.5}\text{Zr}_{0.5}\text{O}_2$ films with TiN electrodes.

The polarization responses from these films have been compared according to their processing temperatures. This comparison reveals that the remanent polarization can vary by up to a factor of 5 for a given processing condition. This is a surprising result provided that the films are nominally structurally identical and points to the possibility that there are additional processing-related differences that impact ferroelectric response. As recently shown by Kim, *et al.*, the stress of a TiN electrode can have a large impact on the phase assemblage and remanent polarization.¹⁵ It was found that by depositing progressively thicker tensile stress top electrodes that the monoclinic phase fraction decreased and the polarization increased. While successful in demonstrating a means to increase ferroelectric phase stability by altering stress imparted by the electrode, the necessity of using micron scale thickness electrodes may not be attractive from a device development and manufacturing perspective. In this work, we sought to understand the interplay of electrode stress on phase assemblage and performance by fixing the electrode thickness at 100 nm and varying its stress by altering the background pressure during sputter deposition. The phase assemblage, polarization response, film stress, and electrode stoichiometry were all characterized. The results of this study will reveal that electrode stoichiometry is also an important variable impacting the phase and performance of hafnium oxide-based ferroelectric films.

2. EXPERIMENTAL PROCEDURES

100 nm thick TaN electrodes were deposited via pulsed DC (30 kHz) magnetron sputtering within a Denton Discovery 550 system onto silicon wafers from a sintered TaN target to form bottom electrodes. Sputter power was kept fixed for all depositions, but the background pressure was varied by controlling the argon flow rate into the sputter system. 20 nm thick $\text{Hf}_{0.5}\text{Zr}_{0.5}\text{O}_2$ films were prepared by thermal atomic layer deposition within an Ultratech Savannah instrument using H_2O as an oxidant and a deposition temperature of 150 °C. After HZO deposition, 100 nm of TaN was deposited and the TaN/HZO/TaN/Si structure was annealed within a rapid thermal annealer to 600 °C for 30 s with a dynamic N_2 atmosphere. Platinum top contacts were defined by photolithography and a lift-off approach and were used as a hard mask to etch the TaN and define discrete capacitors. TaN etching was performed using reactive ion etching, as described in a prior publication.¹⁸ In this study, only the bottom electrode stress was varied. The top electrode stress was kept in a near neutral state (-43 MPa). Note also that reported electrode stresses are the as-deposited stresses measured by wafer flexure.

Film phase assemblage was assessed using grazing incidence X-ray diffraction with a Rigaku SmartLab instrument using $\text{Cu K}\alpha$ radiation. Polarization response was measured with a Radiant Technologies Precision LC instrument using a positive-up, negative-down (PUND) method with a 1 ms pulse and 100 ms delay. Wake-up cycling was performed with 120 Hz square waves. Leakage currents were measured using a Keysight 2901A source measure unit. X-ray photoelectron spectroscopy was performed within a PHI Versaprobe III instrument with monochromated $\text{Al K}\alpha$ radiation. $\text{Sin}^2\psi$ X-ray diffraction experiments were performed on a Panalytical

X'pert instrument.

3. RESULTS AND DISCUSSION

Figure 2 shows remanent polarization as a function of electrode stress in the pristine (open circles) and awoken (closed circles) conditions. It can be observed that films prepared with the most compressive stress displayed the highest remanent polarization in the pristine state. Upon wake-up cycling, all remanent polarization values increase, however the films with the most tensile electrode stress increase the most. The result after wake-up cycling is maximum polarization for the most extreme electrode stress states, regardless of stress sign. This observation is at odds with prior reports showing that compressive stresses result in minimized polarizations while tensile stresses maximize polarization.¹⁰

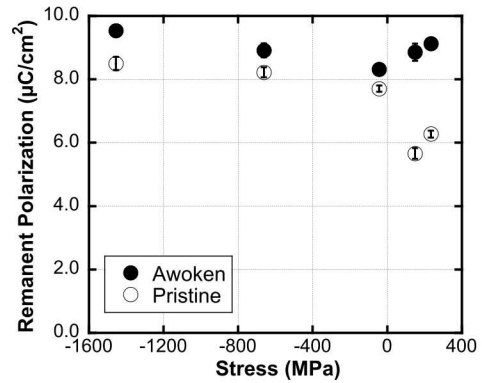


Fig. 2: Remanent polarization as a function of electrode stress in the pristine (as-prepared) and awoken conditions.

Figure 3(a) shows grazing incidence X-ray diffraction patterns of the HZO films. Each film is mixed phase with presence of monoclinic phases (peaks at $\sim 28.5^\circ$ and 31.6° in 2-theta) and a peak that can be attributed to a tetragonal and/or orthorhombic phase at $\sim 30.4^\circ$. While the peak intensities for the phases present appear similar for each film, peak fitting was performed to provide a quantitative assessment. The low angle monoclinic peak and the tetragonal/orthorhombic peak were fit using LIPRAS peak fitting software.¹⁹ The ratios of the tetragonal/orthorhombic to monoclinic peak intensities are compared as a function of electrode stress in Figure 3(b). The results show a similar dependence of phase ratios with electrode stress as the woken-up polarization response. This similarity demonstrates that the reason for the polarization trend observed is due to phase assemblage differences (i.e. reduced monoclinic phase fractions in films with the most stressed electrodes). The observed trend, however, remains inconsistent with prior observations of compressive stresses resulting in reduced responses.

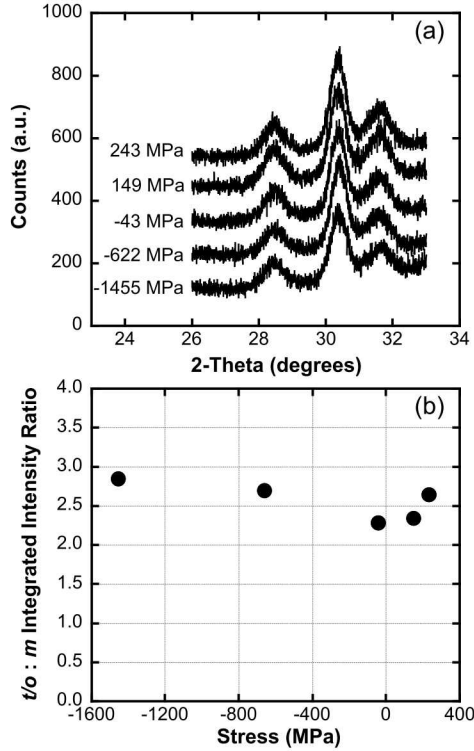


Fig. 3: (a) Grazing-incidence X-ray diffraction patterns of HZO films with differing electrode stress levels. (b) Ratios of the integrated intensities of the tetragonal/orthorhombic:monoclinic peaks.

To assess whether the stresses in the films differ substantially, a $\sin^2\psi$ X-ray diffraction measurement was performed on the tetragonal/orthorhombic peaks. Figure 4 shows the d -spacing of the tetragonal/orthorhombic peaks as a function of $\sin^2\psi$ for the film with the most compressive electrode (-1455 MPa) and that with near-neutral (-43 MPa) electrode stress. In such a representation, a negative slope would indicate a compressive stress and a positive slope a tensile stress. In both cases, a nearly zero slope is observed, suggesting that the stress is nearly neutral in each of these HZO films. This data suggests that film stress is not significantly impacting the phases present or the polarization response in these films.

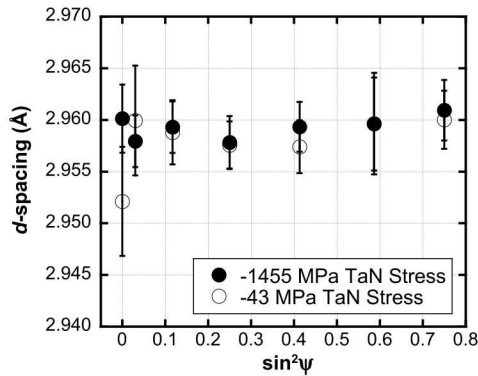


Fig. 4: $\sin^2\psi$ dependence of d -spacing for HZO with -1455 MPa TaN stress (closed circles) and -43 MPa TaN stress (open circles).

Varying background pressure during sputter deposition holds the possibility of altering the TaN film stoichiometry. X-ray photoelectron spectroscopy was performed on witness TaN electrodes across the entire stress series to quantify the Ta:N ratio in the electrodes to determine if composition varied, which could affect the film performance. Figure 5 shows the Ta:N ratio as a function of film stress in the TaN films.

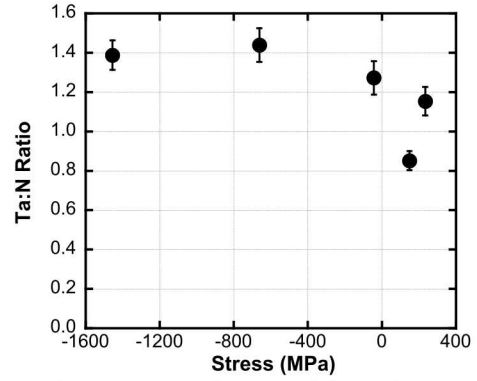


Fig. 5: Ta:N ratio as a function of electrode stress.

It has been observed that the films with the largest compressive stress possess the highest degree of non-stoichiometry and are rich in tantalum. The TaN films with nearly neutral stress are closer to stoichiometric. The shape of the Ta:N ratio and stress dependence is similar to that observed in the polarization and phase assemblage dependence on stress and would suggest a correlation. A possible mechanism by which TaN non-stoichiometry could affect phase assemblage in the HZO films is a reaction of the electrode with the film. Such a reaction could involve oxidation of the TaN electrode at the interface with HZO and result in a reduction of oxygen content in the HZO, *i.e.* forming oxygen vacancies within the HZO film. As oxygen vacancies are suggested to affect phase stability, with more oxygen vacancies resulting in increased stability of higher symmetry phases, such as $Pca2_1$ and tetragonal, such a mechanism appears plausible in this work.

Increased oxygen vacancy content may be expected to lead to increased leakage currents. Leakage current measurements were performed for the stress series films and the results measured with a field of 2 MV/cm are shown in Figure 6 as a function of electrode stoichiometry. It can be seen that for films with electrodes nearest to stoichiometric, which were those that possessed the lowest phase fractions of tetragonal/orthorhombic phases and also displayed the lowest remanent polarizations, the leakage current is the lowest. Low leakage current would be consistent with low oxygen vacancy concentrations. Films prepared on electrodes that were the most non-stoichiometric possessed the highest leakage currents. The most non-stoichiometric TaN films were those that were most stressed, either compressive or tensile. These non-stoichiometric TaN electrodes appear to result in the most oxygen vacancies in the HZO films, which in-turn stabilize a ferroelectric phase preferentially over the equilibrium monoclinic phase and display the largest remanent polarizations.

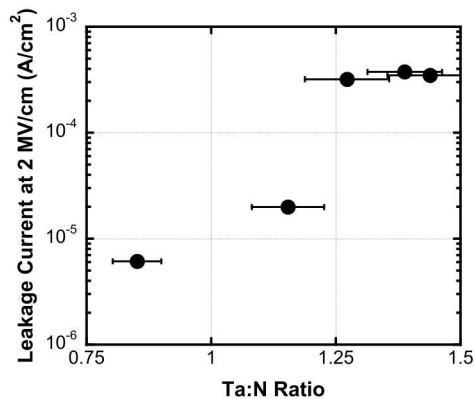


Fig. 6: Leakage current in 20 nm thick HZO films measured at 2 MV/cm versus Ta:N ratio in the bottom electrode.

4. SUMMARY

Electrode processing conditions are shown to impact the phase assemblage and polarization response of hafnium zirconium oxide thin films. Devices prepared with the most stressed TaN electrodes, either compressive or tensile stress, possess the lowest phase fractions of monoclinic phase and display the highest remanent polarizations. The stress of the HZO films is shown to be minimally affected by the stress of the electrode, which suggested that stress was not the primary factor affecting phase assemblage and polarization response. X-ray photoelectron spectroscopy studies of TaN electrode composition revealed that Ta:N ratio was sensitive to the deposition conditions. The films with the most compressive stress had the highest Ta:N ratio and were tantalum-rich. TaN electrodes with near-neutral stress were also the most stoichiometric. HZO polarization response correlated with TaN non-stoichiometry with the largest polarization values recorded for films prepared on the most non-stoichiometric electrodes. The leakage currents of the HZO films scaled with Ta:N ratio. The highest Ta:N ratio electrodes resulted in the highest leakage currents, which can be explained by films having the highest oxygen vacancy concentrations as a result of reaction with the TaN electrodes. As oxygen vacancies are known to stabilize the ferroelectric phase, this work suggests that nitride electrode stoichiometry is a strong factor affecting phase assemblage and polarization response of HZO films.

ACKNOWLEDGEMENTS

This work is supported by the Laboratory Directed Research and Development Program at Sandia National Laboratories. Sandia is a multi-mission laboratory managed and operated by National Technology & Engineering Solutions of Sandia, LLC, a wholly owned subsidiary of Honeywell International, Inc., for the U.S. DOE's National Nuclear Security Administration under contract DE-NA-0003525. The views expressed in the article do not necessarily represent the views of the U.S. DOE or the United States Government. Additional support was provided by faculty startup funds at the University of Virginia.

5. REFERENCES:

[1] T. S. Boscke, J. Muller, D. Brauhaus, U. Schroeder and

U. Bottger, *Appl. Phys. Lett.*, **99** (10), 102903 (2011).

[2] K. J. Hubbard and D. G. Schlom, *J. Mater. Res.*, **11** (11), 2757-2776 (1996).

[3] C. Richter, T. Schenk, M. H. Park, F. A. Tschartke, E. D. Grimley, J. M. LeBeau, C. Zhou, C. M. Fancher, J. L. Jones, T. Mikolajick and U. Schroeder, *Adv. Electron. Mater.*, **3** (10), 1700131 (2017).

[4] U. Schroeder, C. Richter, M. H. Park, T. Schenk, M. Pesic, M. Hoffmann, F. P. G. Fengler, D. Pohl, B. Rellinghaus, C. Zhou, C. C. Chung, J. L. Jones and T. Mikolajick, *Inorg. Chem.*, **57** (5), 2752-2765 (2018).

[5] M. Hoffmann, U. Schroeder, T. Schenk, T. Shimizu, H. Funakubo, O. Sakata, D. Pohl, M. Drescher, C. Adelmann, R. Materlik, A. Kersch and T. Mikolajick, *J. Appl. Phys.*, **118** (7), 072006 (2015).

[6] J. Müller, U. Schröder, T. S. Böske, I. Müller, U. Böttger, L. Wilde, J. Sundqvist, M. Lemberger, P. Kücher, T. Mikolajick and L. Frey, *J. Appl. Phys.*, **110** (11), 114113 (2011).

[7] J. Muller, T. S. Boscke, U. Schroeder, S. Mueller, D. Brauhaus, U. Bottger, L. Frey and T. Mikolajick, *Nano Lett.*, **12** (8), 4318-4323 (2012).

[8] T. Shiraishi, S. Choi, T. Kiguchi, T. Shimizu, H. Funakubo and T. J. Konno, *Appl. Phys. Lett.*, **114** (23), 232902 (2019).

[9] R. Materlik, C. Kuenneth and A. Kersch, *J. Appl. Phys.*, **117** (13), 134109 (2015).

[10] T. Shiraishi, K. Katayama, T. Yokouchi, T. Shimizu, T. Oikawa, O. Sakata, H. Uchida, Y. Imai, T. Kiguchi, T. J. Konno and H. Funakubo, *Appl. Phys. Lett.*, **108** (26), 262904 (2016).

[11] D. Zhou, J. Müller, J. Xu, S. Knebel, D. Bräuhaus and U. Schröder, *Appl. Phys. Lett.*, **100** (8), 082905 (2012).

[12] T. Mimura, T. Shimizu and H. Funakubo, *Appl. Phys. Lett.*, **115** (3), 032901 (2019).

[13] P. Polakowski and J. Müller, *Appl. Phys. Lett.*, **106** (23), 232905 (2015).

[14] S. Starschich, T. Schenk, U. Schroeder and U. Boettger, *Appl. Phys. Lett.*, **110** (18), 182905 (2017).

[15] S. J. Kim, D. Narayan, J.-G. Lee, J. Mohan, J. S. Lee, J. Lee, H. S. Kim, Y.-C. Byun, A. T. Lucero, C. D. Young, S. R. Summerfelt, T. San, L. Colombo and J. Kim, *Appl. Phys. Lett.*, **111** (24), 242901 (2017).

[16] M. H. Park, H. J. Kim, Y. J. Kim, W. Jeon, T. Moon and C. S. Hwang, *Phys. Status Solidi R*, **8** (6), 532-535 (2014).

[17] M. H. Park, H. J. Kim, Y. J. Kim, W. Lee, T. Moon and C. S. Hwang, *Appl. Phys. Lett.*, **102** (24), 242905 (2013).

[18] S. W. Smith, A. R. Kitahara, M. A. Rodriguez, M. D. Henry, M. T. Brumbach and J. F. Ihlefeld, *Appl. Phys. Lett.*, **110** (7), 072901 (2017).

[19] G. Esteves, K. Ramos, C. M. Fancher, and J. L. Jones. LIPRAS: Line-Profile Analysis Software. (2017). DOI: 10.13140/RG.2.2.29970.25282/3.